Science Forum (Journal of Pure and Applied Sciences)

Journal Homepage: https://atbu.edu.ng/science-forum/

SIMULATION OF NON-EQUILIBRIUM FLOWS USING LATTICE BOLTZMANN METHOD

[1]Ehigbor L. O, [2]Nagwai A. P, [3] Braimah L. S[3], [4]Usman N. M

[1]Shagofomi Tide Limited, 16 Mbonu Street Dline, Port Harcourt, Rivers State

[2]British American Business and Management School, Port Harcourt Campus

[3]Logistics Department, National Inland Waterways Authority Outer Marina, Ferry Terminal CMS, Lagos

[4]Husmanasirsat Nigeria limited. No 1 Kachia Road, Kaduna

ABSTRACT

In this work, non-equilibrium flows were studied using the lattice Boltzmann method: (1) laminar to turbulent by-pass transition on a flat-plate at high upstream turbulent intensity (6%) (2) boundary layer development on a NACA0012 airfoil for various angles of attack (3◦, 4.5◦ and 6◦) using large eddy simulations. Numerical simulations are performed using the transient and compressible lattice Boltzmann solver SIMULIA PowerFLOW. The transition to turbulence on the flat-plate and the separation bubble size and locations on the airfoil with varying flow conditions are captured well and in close validation with literature. Future works involve running airfoil cases at different upstream turbulent intensity.

NOMENCLATURE

$U\infty$ = Free stream inlet velocity
Cp = pressure coefficient
CL = Lift coefficient
Cf = Skin friction
c = airfoil chord length
L = plate length
Rec = Reynolds number based on chord length and free stream velocity
ν = kinematic viscosity
$\delta\nu$ = viscous length scale
$u\tau$ = friction velocity
ωz = span-wise vorticity

ARTICLE INFO

Received 11 July 2023
Received in Revised Form 10 August 2023
Accepted 11 August 2023
Published xxxxxxx
Available online

KEYWORDS

Non-Equilibrium Flows,
Lattice Boltzmann,
Upstream,

I. Introduction

Most flows encountered in industrial application are non-equilibrium in nature. By non-equilibrium, it means flows are non-self-similar i.e. statistics cannot be normalized in a way that it can be independent of its stream-wise location. Such flows include laminar to turbulent transitions, flows with separation bubbles, boundary layer flows with varying favourable and adverse pressure gradients the along stream-wise direction induced by flow conditions or wall curvature etc. Understanding such flow scenarios find its applications in several industries such as aerospace (airplanes and space-crafts), oil and gas (pipe flows etc.), automotive, HVAC etc. This explains them being some of the popular areas of research in fluid mechanics in the past decades.

Laminar to turbulent transition has been studied by several researchers in the past century. As reviewed in detail by Saric et al. [1] , this process either goes through several stages: receptivity process i.e. initial weak disturbances

*Corresponding Author L. O. Ehigbor ✉ apnagwai@gmail.com ✉ Shagofomi Tide Limited, 16 Mbonu Street Dline, Port Harcourt, Rivers State

in the flow due to such as sound or vorticity, followed by primary instabilities and then secondary instabilities involving three-dimensional non-linear interactions, and then these disturbances rapidly leads to turbulence; or skipping the whole transient growth of linear disturbances with high enough initial turbulent intensity, with turbulent spots occurring randomly, to directly transitioning to turbulence, called by-pass transition [2, 3]. This work focuses on the by-pass transition. Several researchers have studied this process in detail experimentally as well as numerically. Jacobs and Durbin [4] based on DNS results, reported the formation of long stream-wise backward jets i.e. low speed streaks neathe wall. These large stream-wise structures interact with free stream eddies, which leads to generation of turbulent spots. Similarly, Brandt et al. [5] carried out DNS simulations and found elongated regions of high and low stream-wise velocity, which later due to local instabilities, become unstable and break to form turbulent spots. In recent years, researchers are heading towards finding transition markers to come up with models, for better transition predictions.

Several models have been developed in the past for the transition. Such as turbulent potential model proposed by Wang and Perot [6], correlation-based transition model by Langtry and Menter [7] , to name a few. Additionally, various active research areas pertaining to such flow scenarios, including but not limited to are: transition due to surface roughness [8 , 9], quasi-laminarization due to accelerations [10], transition in the presence of drag reducing surfaces such as riblets[11], transition in laminar separation bubble (such as on airfoil's suction side) and several others.

Laminar separation bubble (LSB) is one of the crucial aspects in boundary layer flows over airfoils, as it effects lift and drag coefficients to a great extent. Such flow conditions are pretty evident in micro air vehicles (MAV) or unmanned air vehicles (UAVs), as they have smaller chord length and comparatively slow speed as compared to commercial aircrafts [12]. Hence, several researchers have carried out experiments as well as high fidelity numerical simulations to understand boundary layer development on airfoils at such a low Reynolds number Rec< 1e6 (based on the airfoil chord length). Tsuchiya et al. [13] conducted experiments at the Mars wind tunnel of Tohoku University, to understand the effect of turbulence intensity on flow development on the NACA0012 airfoil at Rec< 50, 000. Results indicatedthat with the increase of upstream turbulent intensity, lift increased at low angles of attack, whereas drag decreasedfor all angles of attack. Similarly, Zhang et al. [14] showed that higher turbulence intensity or Reynolds number leads to larger stalling angle and early transition, based on URANS simulation carried out on NACA0012 and SD7037. Li et al. [15] carried out DNS simulations as well experimental measurements at a much lower Rec = 5300, and found that stall does not occur at low turbulence intensity but occur at high turbulence intensity. Balakumar [16] calculated the development of higher order turbulent statistics such as turbulent diffusion, advection and dissipation terms along the chord as boundary layer develops on the NACA0012 airfoil at low to moderate Reynolds numbers, based on DNS simulation. Lee et al. [17] examined the efficacy of different numerical methods such as RANS, 2D/3D LES to predict aerodynamic characteristics of the NACA0012 airfoil. It was found that RANS was unable to reproduce the boundary layer development, whereas 2D LES can predict the results qualitatively. They recommended high fidelity simulations like 3D LES for more accurate analysis.

Not limiting to aerodynamic characteristics, researchers have carried out in-depth analysis to understand feedback mechanism in trailing edge noise on airfoils in such flow conditions, relevant to applications in fans, UAVs and wind turbines. Plogmann et al. [18] carried out experiments on the NACA0012

airfoil at a Reynolds number around 1e5 at various angles of attack using the coherent velocity method, to study the discrete frequency tones in the trailing edge noise spectra. Pröbsting et al. [19] investigated the tonal noise generation using the particle image velocimetry (PIV) for the NACA0012 airfoil at various angles of attack. Results attributed tone generation to vertical structures formed from shear-layer instabilities. Also, similar analysis was done [20] at low to medium Reynolds numbers, and it was found that tonal noise general depends on suction side boundary layer events at low Reynolds numbers, and dominated by pressure side at higher Reynolds numbers. Ricciardi et al. [21] , based on LES and linear stability analysis of the NACA0012 airfoil at Rec = 50, 000, investigated secondary tones and acoustic feedback mechanism. The plethora of research conducted in such complex flow scenarios suggests the importance of high fidelity simulations required to study the flow physics in detail.

In this paper, the efficacy of lattice Boltzmann method based on the SIMULIA PowerFLOW solver will be demonstrated to capture the flow physics of such transient conditions. The paper is organized as follows. Section II introduced the numerical method, the lattice Boltzmann framework and turbulence boundary treatments. Section III presented results for the boundary layer by-pass transition on a flatplate with 6% turbulent intensity at the leading edge, as well as the formation of laminar separation bubble on the suction side pf the NACA0012 airfoil at Re = 50, 000 with different angles of attack. Section IV briefly concludes this study and future works.

II. NUMERICAL METHOD

The lattice Botzmann method is adopted in this study and the state-of-the-art high-fidelity LB solver, the SimuliaPowerFLOW is used. In this numerical method, the Boltzmann equation was discretized in both time space and velocity space by D3Q19 lattices (3 dimensions 19 states), and the regularized lattice Boltzmann equation with the filtered collision satisfying the Garlilean invariance shown in Eq. (1) by Chen et al. [22] was solved numerically.

$$f_i(x + c_i\delta_t, t + \delta t) = f_i^{eq}(x,t) + \left(1 - \frac{1}{\tau}\right) f_i^{eq}(x,t) \quad (1)$$

The discrete equilibrium distribution function f_i^{eq} can be obtained through the Hermite series expansion [23], while the expression of filtered non-equilibrium distribution f_i^{neq} can be found in [22]. The macroscopic quantities such as the mass density ρ and the momentum density ρu, can be computed through the moments of the particle distribution functions $f_i(x,t)$:

$$\rho(x,t) = \sum_i f_i\,(x,t) \quad (2a)$$

$$\rho(x,t) \cup (x,t) = \sum_i c_i f_i\,(x,t) \quad (2b)$$

A separate macroscopic equation for energy is solved by an LB approach which satisfying the exact energy conservation [24, 25]:

$$\frac{\partial \rho E_t}{\partial t} + \nabla.[(\rho E_t + p)u] = \nabla.(k\nabla T) + \nabla.(u.\boldsymbol{\tau}) \quad (3)$$

Here $E_t = C_v T + \frac{|u|^2}{2}$ is the total energy and $\boldsymbol{\tau}$ is the strain rate tensor. The momentum solver and energy solver are properly coupled such that correct thermodynamics are ensured [26 ,27]. More details about the LBM methodology for high speed flows can also be found in [27, 28].

The simulations are carried out using an implicit large-eddy simulation approach, where the inviscid energy i.e. the inertial range of turbulent cascade is solved by the numerical method, and the numerical dissipation acts as a sub-grid scale model [29]. For the wall function, pressure gradient effects are modelled into the standard wall model, using near wall unresolved length scale, wall shear stress and pressure gradient along the wall curvature [29]. The LBM solver uses cubic elements called voxels for volume discretization. Variable resolutions (VR) are

defined in flow domain to have higher resolution in region of interests. More details on the method and solver can be found in Romani et al. [29].

III. RESULTS AND DISCUSSIONS

A. Laminar to Turbulent Transition on a Flatplate

For the flatplate case, the Reynolds number based on the length of plate (l) and the free-stream velocity U_∞ is 1e6, with a Mach number of Ma = 0.2. At the inlet, U_∞ is applied in the $x$direction. While at the outlet, the ambient pressure (P = 101325 Pa) is applied. Periodic boundary conditions were applied in the span-wise direction (with a size of 0.1l) of the flatplate. At the flatplate wall, the no-slip boundary condition was used, with an initial frictionless wall (slip wall) between the inlet and the flatplate, as shown in Fig. 1. There are totally 6 Variable Resolution (VR) levels from 0 to 5.

A higher VR level means a finer voxel size. The minimum voxel size in VR 5 is 1.25 mm.

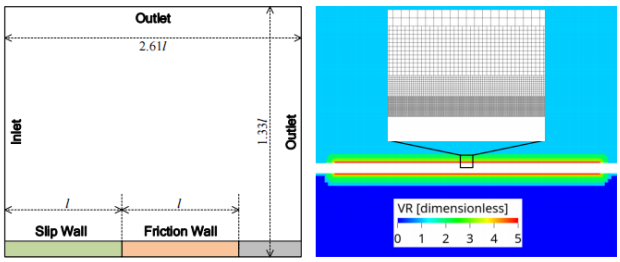

Fig. 1 Illustration of computations setup and grid for the flatplate case (not drawn to scale). There are totally 6 Variable Resolution (VR) levels from 0 to 5. The minimum voxel size in VR 5 (wall resolution) is 1.25 mm. ($yw+ < 1$)

The by-pass transition goes through three phases: buffeted laminar boundary layer, formation of turbulent spots, and transition to fully developed turbulent boundary layer, as thoroughly discussed by Jacobs and Durbin [4]. In the buffeted laminar stage, boundary layer is predominantly stable, with low speed streaks getting elongated in the stream-wise direction near the wall. At this point, the skin friction Cf magnitude is still low, approximately same as for a laminar boundary layer, but slightly higher. Then, localized 3D irregularities are generated called turbulent spots, which disturb the elongated low speed streaks. At this point, Cf reaches towards a point of local minima, following which Cf starts increasing towards fully developed turbulent boundary layer at the last stage. As these elongated streaks become unstable, they break to form smaller highly 3-dimensional smaller turbulent structures; leading to transition to fully developed turbulent boundary layer.

As observed previously by several researchers and discussed briefly above, skin friction is one of the main transition markers, which is sensitive to the boundary layer transition. Hence, we compare the variation of Cf to validate against published results. As shown in Fig. 2, results are compared with the experimental data [30] for flat plate boundary layer with upstream turbulent intensity of 6% at flat-plate leading edge. The overall variation of Cf is captured well by the LBM solver Power FLOW, i.e. three stages: decrease in , reaching a point of minima at approximately same $Rex \approx 60000$, and transiting to the fully turbulent state. A slight delay is seen towards the end, which can be attributed to a bit lower upstream turbulent intensity at leading edge as compared to experiments. In the LES study conducted by Voke and Yang [31] , there is a bit earlier start to transition, and also its local minima is quite far from the experimental results. When it comes to transition models, potential model [6] comes closest to transition prediction. Still its critical transition point is bit delayed $Rex \approx 75000$, and also Cf local minima is higher in comparison to experimental results.

Similar results are seen for $\gamma - Re\theta$ RSM model [32]. Whereas for the $\gamma - Re\theta$[7], the critical transition location is similar to experimental data, but Cf is magnitude is much higher for the whole transition process.

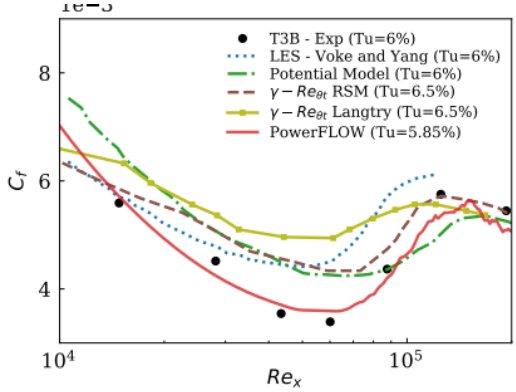

Fig. 2 Laminar to turbulent by-pass transition for boundary layer with zero pressure gradient on a flat plate with 6% turbulent intensity.

Overall, all the cases i.e. LES and transition models, show the Cf trend as seen in the by-pass transition, but the PowerFLOW solver comes closest in capturing the critical transition location and Cf local minima, as well as its overall variation, for the case in consideration.

B. LAMINAR SEPARATION ON THE NACA0012

The NACA-0012 airfoil is simulated to capture the variation and location of laminar separation bubble with different angles of attack (3◦, 4.5◦ and 6◦). For this case, the Reynolds number is 50,000 based on the chord-length (c) and the free-stream velocity $U\infty$, with a Mach number of Ma = 0.2. And $U\infty$ is applied at the inlet (turbulent intensity <0.1%) with the static pressure (p) applied at the outlet. The No-slip boundary was applied at the airfoil surface. Periodic boundary conditions were applied on the sides with a span of 0.1c. The details are illustrated in Fig. 3. To capture the transition and laminar separation bubble,the wall normal resolution near the wall ($y+ = yv/$) is kept of the order 1. A total of 7 VRs are used for the airfoil case.

At the given low Reynolds number, the boundary layer developed on the suction side is laminar, until it reaches the laminar separation bubble. Starting from the leading edge because of the angle of attack and the curvature, the adverse pressure gradient appeared as the boundary layer is developed, leading to fast reduction in the , until the laminar boundary separation. Following the separation, at some downstream location, separated shear layer transitions into turbulent, and then reattaches itself with the wall. So, the separated laminar boundary layer, followed by laminar to turbulent transition and then reattachment to form fully developed boundary layer, forms a “bubble”, which is called the laminar separation bubble (LSB) [33–36].

With the increase in the angle of attack, LSB goes from near the trailing edge at 3◦ (Fig. 4), to towards the leadingedge at 6◦ (Fig. 6). Also the size of bubble decreases, with the increase in the angle of attack. The LSB signature is alsoreflected in the wall pressure coefficient, where it reaches a stable constant value, following separation, followed by aabrupt dip in transition range

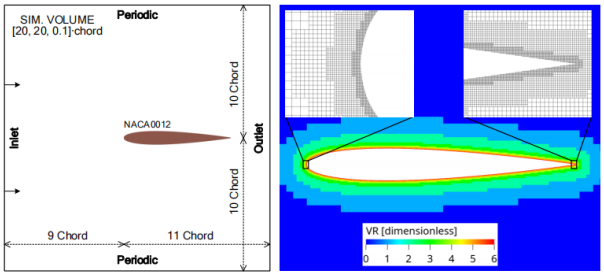

Fig. 3 Illustration of computations setup and grid for the NACA0012 case (not drawn to scale). There are totally 7 Variable Resolution (VR) levels from 0 to 6. The minimum voxel size (wall resolution) in VR 6 is 0.16mm.($yw+ \approx 1$)

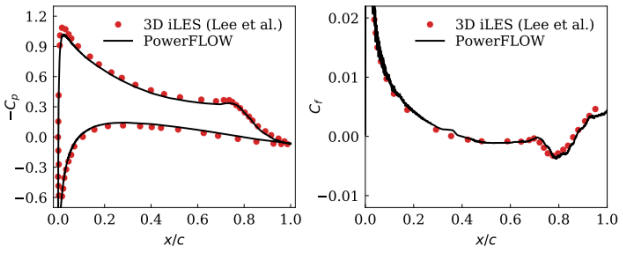

Fig. 4 Pressure and friction coefficients for angle of attack 3.0◦ at Re = 5×104.

Overall, the comparison of Cf and Cp with Lee et al. [17] , for different angles of attack, suggest that the size and the location of the LSB are captured accurately by the PowerFLOW LBM solver.

Next in Fig. 7, lift and drag coefficient variation with angles of attack is compared with

experimental data [37]. Results from PowerFLOW show improvement in load coefficient for angles of attacks 3◦ and 4.5◦, as compared to Lee et al. [17], whereas drag coefficient is in close comparison with Lee's [17] results.

The wall-normal profiles of the stream-wise velocity are shown in Fig. 8. Following separation, inflection points are observed between chord locations x/c = 0.4, 0.8 for 3◦, x/c = 0.4, 0.6 for 4.5◦ and at x/c = 0.2, 0.4 for 6◦, whichsuggests strong flow reversal in the LSB region. Due to the long LSB region, the laminar to turbulent transition and the strong adverse-pressure gradient (APG), that are induced due to the curvature and the angle of attack, the log-law isn't established following re-attachment.

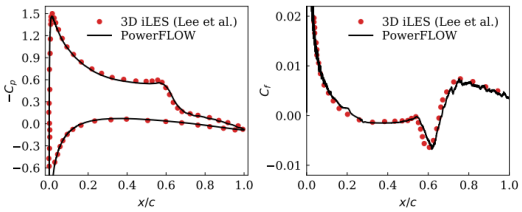

Fig. 5 Pressure and friction coefficients for angle of attack 4.5° at Re = 5×10^4.

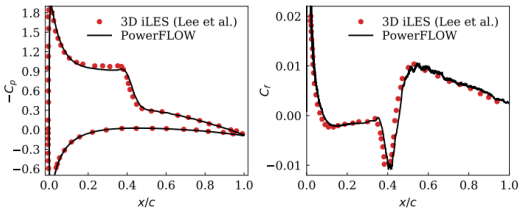

Fig. 6 Pressure and friction coefficients for angle of attack 6.0° at Re = 5×10^4.

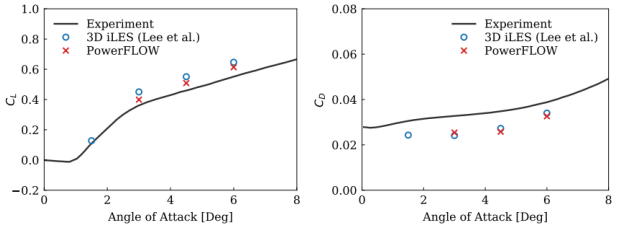

Fig. 7 Lift coefficients for different angles of attack at Re = 5×104.

In Fig. 9 (a), the instantaneous span-wise vorticity is shown using iso-surfaces for 3◦ angle of attack. Up-till x/c = 0.72, boundary layers are predominantly 2D laminar, even after separation at $x/c\approx$ 0.2. Then near the transition,

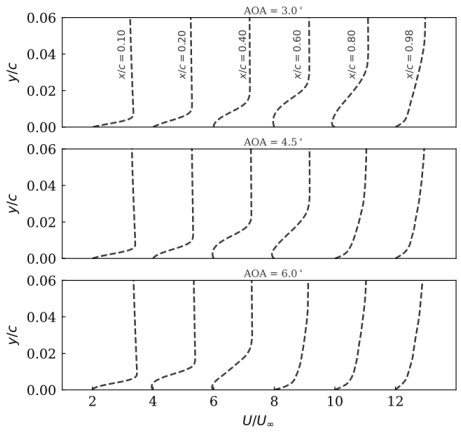

Fig. 8 Wall-normal variation of time averaged stream-wise velocity at various chord locations for angle of attack 3.0◦ (top), 4.5◦ (middle) and 6.0◦ (bottom). disturbances are seen in the shear layer, followed by breakdown to 3D turbulent structures in the transition regime, with boundary layer fully turbulent in the transition regime.

Then in Fig. 9 (b,c,d) iso-surfaces of stream-wise, wall-normal and span-wise fluctuations are shown. Disturbances in stream-wise and wall-normal fluctuations are observed near initial distortions, whereas for span-wise fluctuations, they start in the transition regime. These fluctuations are only seen in the vicinity of transition and following reattachment. This supports the fact that boundary layer is predominant laminar prior to transition, even after flow separation.

IV. CONCLUSION AND FUTURE WORKS

Large eddy simulations are carried out using the lattice Boltzmann solver SimuliaPowerFLOW, to capture the turbulent dynamics of non-equilibrium flows: (1) by-pass transition on a flat plate and (2) low-Re boundary layer flow over the NACA-0012 airfoil with different angles of attack. For the flat plate case, Power FLOW captures the transition in close approximation to experimental results. The overall variation of , and critical transition locations are validating well with experiments, better than other published results and transition models. When it comes boundary layer development over the NACA0012 airfoil, with varying angles of attack,

the size and location of LSB is overlapping well with published works. Variation of stream-wise velocity profile along wall normal direction, at different stream-wise locations, shows the strong flow reversal due to the adverse pressure gradient applied due to the curvature and the angle of attack. The isosurfaces of instantaneous span-wise vorticity and turbulent fluctuations show that the boundary layer is predominantly laminar, even after flow separation, and transitions to turbulence, towards the end of LSB. In general, results are overlapping well with references considered, and the non-equilibrium flow physics is in line with published literature.

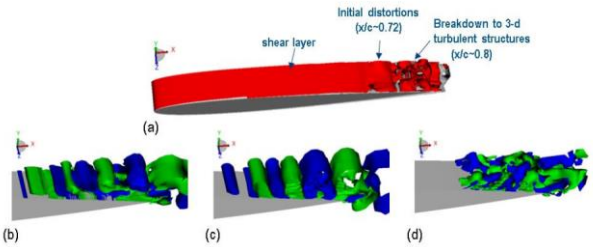

Fig. 9 Isosurfaces of (a) instantaneous span-wise vorticity ($\frac{\omega Zc}{U_\infty} = 30$ *(red); -30(grey)) (b) instantaneous stream-wise fluctuations* $\frac{u'}{U_\infty} = \pm 0.05$ *(c) instantaneous wall-normal fluctuations* $\frac{v'}{U_\infty} = \pm 0.02$*(d) instantaneous span-wise fluctuations* $\frac{\omega'}{U_\infty} = \pm 0.03$*(positive- blue, negative- green) for NACA-0012 with 3 degrees angle of attack*

For future works, we plan to carry out the transition simulation with lower to minimal turbulent intensity, to gauge the solver's ability to capture near-wall physics in laminar to turbulent transition i.e. receptivity processes, primary and secondary growth and then transition. Also, for the NACA0012 airfoil, simulations will be carried out with higher turbulent intensities to check how LSB size and location varies for different angles of attack.

REFERENCES

[1] Saric, W. S., Reed, H. L., and Kerschen, E. J., "Boundary-layer receptivity to freestream disturbances," Annual review of fluid mechanics, Vol. 34, No. 1, 2002, pp. 291–319.

[2] Morkovin, M. V., "On the many faces of transition," Viscous drag reduction, Springer, 1969, pp. 1–31.

[3] Morkovin, M. V., "Bypass-transition research: issues and philosophy," Instabilities and Turbulence in Engineering Flows, Springer, 1993, pp. 3–30.

[4] Jacobs, R., and Durbin, P., "Simulations of bypass transition," Journal of Fluid Mechanics, Vol. 428, 2001, pp. 185–212.

[5] Brandt, L., Schlatter, P., and Henningson, D. S., "Transition in boundary layers subject to free-stream turbulence," Journal of Fluid Mechanics, Vol. 517, 2004, pp. 167–198.

[6] Wang, C., and Perot, B., "Prediction of turbulent transition in boundary layers using the turbulent potential model," Journal of Turbulence, Vol. 3, No. 1, 2002, p. 022.

[7] Langtry, R. B., and Menter, F. R., "Correlation-based transition modeling for unstructured parallelized computational fluid dynamics codes," AIAA journal, Vol. 47, No. 12, 2009, pp. 2894–2906.

[8] Choudhari, M., Li, F., Chang, C.-L., Edwards, J., Kegerise, M., and King, R., "LLaminar-Turbulent Transition behind Discrete Roughness Elements in a High-Speed Boundary Layer," 48th AIAA aerospace sciences meeting including the new horizons forum and aerospace exposition, 2010, p. 1575.

[9] De Tullio, N., Paredes, P., Sandham, N., and Theofilis, V., "Laminar–turbulent transition induced by a discrete roughnesselement in a supersonic boundary layer," Journal of Fluid Mechanics, Vol. 735, 2013, pp. 613–646.

[10] Piomelli, U., and Yuan, J., "Numerical simulations of spatially developing, accelerating boundary layers," Physics of Fluids, Vol. 25, No. 10, 2013, p. 101304.

[11] Pargal, S., Yuan, J., and Brereton, G., "Impulse response of turbulent flow in smooth and riblet-walled channels to a sudden velocity increase," Journal of Turbulence, Vol. 22, No. 6, 2021, pp. 353–379.

[12] Xiao, T., Li, Z., Deng, S., Ang, H., and Zhou, X., "Numerical study on the flow characteristics of micro air vehicle wings at low Reynolds numbers," International Journal of Micro Air Vehicles, Vol. 8, No. 1, 2016, pp. 29–40.

[13] Tsuchiya, T., Numata, D., Suwa, T., and Asai, K., "Influence of turbulence intensity on aerodynamic characteristics of an NACA 0012 at low Reynolds numbers," 51st AIAA Aerospace Sciences Meeting Including the New Horizons Forum and Aerospace Exposition, 2013, p. 65.

[14] Zhang, Y., Zhou, Z., Wang, K., and Li, X., "Aerodynamic characteristics of different airfoils under varied turbulence intensities at low Reynolds numbers," Applied Sciences, Vol. 10, No. 5, 2020, p. 1706.

[15] Li, S.-w., Wang, S., Wang, J.-p., and Mi, J.-c., "Effect of turbulence intensity on airfoil flow: Numerical simulations and experimental measurements," Applied Mathematics and Mechanics, Vol. 32, No. 8, 2011, pp. 1029–1038.

[16] Balakumar, P., "Direct numerical simulation of flows over an NACA-0012 airfoil at low and moderate Reynolds numbers," 47thAIAA Fluid Dynamics Conference, 2017, p. 3978.

[17] Lee, D., Nonomura, T., Oyama, A., and Fujii, K., "Comparison of numerical methods evaluating airfoil aerodynamic characteristics at low Reynolds number," Journal of Aircraft, Vol. 52, No. 1, 2015, pp. 296–306.

[18] Plogmann, B., Herrig, A., and Würz, W., "Experimental investigations of a trailing edge noise feedback mechanism on a NACA 0012 airfoil," Experiments in fluids, Vol. 54, No. 5, 2013, pp. 1–14.

[19] Pröbsting, S., Serpieri, J., and Scarano, F., "Experimental investigation of aerofoil tonal noise generation," Journal of Fluid Mechanics, Vol. 747, 2014, pp. 656–687.

[20] Pröbsting, S., Scarano, F., and Morris, S., "Regimes of tonal noise on an airfoil at moderate Reynolds number," Journal ofFluid Mechanics, Vol. 780, 2015, pp. 407–438.

[21] Ricciardi, T. R., Wolf, W. R., and Taira, K., "Transition, intermittency and phase interference effects in airfoil secondary tones and acoustic feedback loop," Journal of Fluid Mechanics, Vol. 937, 2022.

[22] Chen, H., Zhang, R., and Gopalakrishnan, P., "Filtered lattice Boltzmann collision formulation enforcing isotropy and Galilean invariance," PhysicaScripta, Vol. 95, No. 3, 2020, p. 034003.

[23] Shan, X., Yuan, X.-F., and Chen, H., "Kinetic theory representation of hydrodynamics: a way beyond the Navier–Stokes equation," Journal of Fluid Mechanics, Vol. 550, 2006, pp. 413–441.

[24] Zhang, R., Fan, H., and Chen, H., "A lattice Boltzmann approach for solving scalar transport equations," Philosophical Transactions of the Royal Society A, Vol. 369, 2011, pp. 2264–2273.

[25] Pradeep Gopalakrishnan, R. Z., and Chen, H., "Lattice Boltzmann solver enforcing

total energy conservation," Patent Pending, 2018.

[26] Nie, X., Shan, X., and Chen, H., "Lattice-Boltzmann / Finite-Difference Hybrid Simulation of Transonic Flow," 47th Aerospace Sciences Meeting including the New Horizons Forum and Aerospace Exposition, 2009, p. 0139.

[27] Li, Y., Jammalamadaka, A., Gopalakrishnan, P., Zhang, R., and Chen, H., "Computation of High-Subsonic and Transonic Flows by a Lattice Boltzmann Method," 54th Aerospace Sciences Meeting, 2016, p. 0043.

[28] Fares, E., Wessels, M., Zhang, R., Sun, C., Gopalaswamy, N., Roberts, P., Hoch, J., and Chen, H., "Validation of a lattice-Boltzmann approach for transonic and supersonic flow simulations," 52nd Aerospace Sciences Meeting, 2014, p. 0952.

[29] Romani, G., Casalino, D., and Velden, W. v. d., "Numerical Analysis of Airfoil Trailing-Edge Noise for Straight and Serrated Edges at Incidence," AIAA Journal, Vol. 59, No. 7, 2021, pp. 2558–2577.

[30] Roach, P., "The influence of a turbulent free-stream on zero pressure gradient transitional boundary layer development: Part 1. Test cases T3A and T3B," ERCOFTAC Workshop, Lausanne, 1990, 1990, p. 0.

[31] Voke, P. R., and Yang, Z., "Numerical study of bypass transition," Physics of Fluids, Vol. 7, No. 9, 1995, pp. 2256–2264.

[32] Nie, S., Krimmelbein, N., Krumbein, A., and Grabe, C., "Coupling of a Reynolds Stress Model with the γ- R e θ t TransitionModel," AIAA Journal, Vol. 56, No. 1, 2018, pp. 146–157.

[33] Gaster, M., The structure and behaviour of laminar separation bubbles, Citeseer, 1967.

[34] Kähler, C. J., "Experimental investigation of flows at low Reynolds number using optical techniques," RTO/AVT, Vol. 104, 2003.

[35] Ol, M., McCauliffe, B., Hanff, E., Scholz, U., and Kähler, C., "Comparison of laminar separation bubble measurements on a low Reynolds number airfoil in three facilities," 35th AIAA fluid dynamics conference and exhibit, 2005, p. 5149.

[36] Ravi, S., "The influence of turbulence on a flat plate aerofoil at Reynolds numbers relevant to MAVs," Ph.D. thesis, RMIT University, 2011.

[37] Ohtake, T., Nakae, Y., and Motohashi, T., "Nonlinearity of the aerodynamic characteristics of NACA0012 aerofoil at low Reynolds numbers," Japan Society of Aeronautical Space Sciences, Vol. 55, No. 644, 2007, pp. 439–445